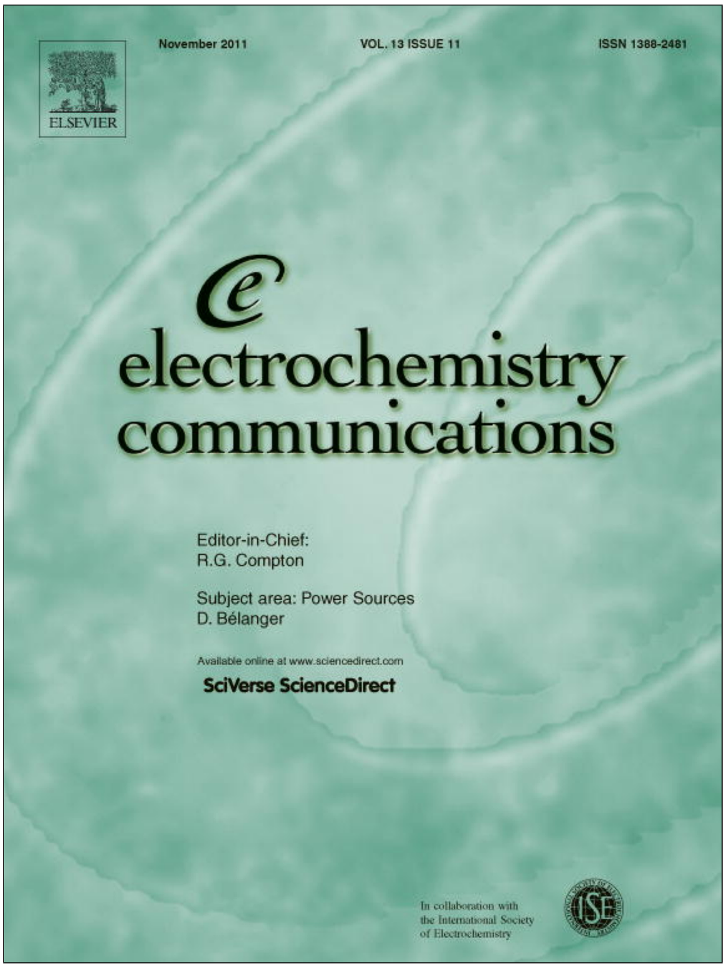
November 2011
VOL. 13 ISSUE 11
ISSN 1388-2481
ELSEVIER
electrochemistry communications
Editor-in-Chief:
R.G. Compton
Subject area: Power Sources
D. Bélanger
Available online at www.sciencedirect.com
SciVerse ScienceDirect
In collaboration with the International Society of Electrochemistry
ISE

Electrochemistry Communications 13 (2011) 1276–1279

Contents lists available at SciVerse ScienceDirect

Electrochemistry Communications

journal homepage: www.elsevier.com/locate/elecom

# Porous nanostructured $V_2O_5$ film electrode with excellent Li-ion intercalation properties

Yanyi Liu [a], Jiangang Li [a,b], Qifeng Zhang [a], Nan Zhou [a,c], Evan Uchaker [a], Guozhong Cao [a,*]

[a] Department of Materials Science and Engineering, University of Washington, Seattle, WA 98195, USA
[b] Department of Applied Chemistry, Beijing Institute of Petrochemical Technology, Beijing 102617, China
[c] College of Chemistry and Chemical Engineering, Central South University, Changsha, Hunan, 410083, China

ARTICLE INFO

*Article history:*
Received 13 July 2011
Received in revised form 12 August 2011
Accepted 12 August 2011
Available online 19 August 2011

*Keywords:*
Vanadium oxide
Porous film
Li-ion battery
$Li^+$ intercalation

ABSTRACT

Porous nanostructured $V_2O_5$ films were prepared by electrodeposition from $V_2O_5$ sol with the addition of block copolymer Pluoronic P123, and they can be readily applied as Li-ion battery cathode without adding any polymer binder or conductive additives. SEM images showed an ideal morphology for $Li^+$ intercalation favored charge transfer kinetics, which is a combination of homogeneously distributed nano-pores and $V_2O_5$ nanoparticles. Electrochemical measurements revealed that, the porous nanostructured $V_2O_5$ films have a high discharge capacity of 160 mAh/g at 9 A/g, and maintain 240 mAh/g after 40 cycles at 300 mA/g. The excellent $Li^+$ intercalation property could be ascribed to the high surface area, sufficient contact between electrode materials and electrolyte, short $Li^+$ diffusion path, as well as the good accommodation for volume change which are benefited from homogeneously distributed nano-pores and $V_2O_5$ nanoparticles.

## 1. Introduction

Li-ion battery has been intensively studied and developed as one of the most successful energy storage technologies for application in portable electronics, and a promising candidate to power hybrid electrical vehicles (HEV) and electrical vehicles (EV) [1]. In spite of the significant progress made in both material science and device technologies, Li-ion batteries are lagging way behind the rapid advancement of electronics and other technologies, which demand higher energy and higher power with longer lifetime. Recent extensive research has demonstrated that appropriately designed and fabricated nanostructured materials with controlled surface chemistry could offer the possibilities to (1) enhance the charge transfer kinetics at electrolyte/electrodeinterface as well as $Li^+$ diffusion process in electrode during $Li^+$ intercalation/deintercalation, (2) increase the Li-ion intercalation capacity with a much increased surface energy facilitating reversible phase transition and (3) attain good mechanical integrity of the electrode materials [2].

There have been a great number of studies on manipulating the nanostructure or surface chemistry of electrode materials to achieve much enhanced charge transfer kinetics and electrical conductivity: adding carbon nano-coatings on $LiFePO_4$, [3] fabricating nanocomposite electrodes composed of graphene or carbon with actives, [4] creating $Li^+$ intercalation favored nanostructures, such as nano-porous, nano-rod/tube/cable [5,6] and introducing surface defects by gas annealing or aliovalent doping [7,8]. In spite of the much enhanced electrochemical properties that have been reported in those literatures, most of the aforementioned nanostructured electrodes require complicated fabrication approaches and high processing costs. In this research, a technically straightforward and low-cost method has been developed to prepare homogeneous and porous nanostructured $V_2O_5$ film electrodes from vanadia sol with the addition of block copolymer. The resulting nano-porous $V_2O_5$ film demonstrates excellent storage capacity, rate capability, and cyclic stability when tested as cathode for Li-ion battery. The nano-porous film formation mechanism, crystallinity, morphology and electrochemical properties were investigated and discussed.

## 2. Experimental

The porous structured $V_2O_5$ films were prepared by electrodeposition following the same procedure as previously reported [9]. $V_2O_5$ powders (99.8%, Alfa-AESAR) were added into de-ionized water and $H_2O_2$ (30 wt.% in $H_2O$, Sigma-Aldrich) at a $V_2O_5$ concentration ($C_V$) of 0.3 M and $n(H_2O_2):n(V)$ of 8.05:1, and the resulting solution was stirred and sonicated for 15 min successively, followed by being diluted to $C_V = 0.06$ M and then sonicated for 1 h until the solution turned into brownish red $V_2O_5$ gel. The block copolymer Pluronic P123 $[(CH_2CH_2O)_{20}–(CH_2CH(CH_3)O)_{70}– (CH_2CH_2O)_{20}]$ was dissolved into de-ionized water to form a transparent 4 wt.% solution, and then mixed with the aforementioned $V_2O_5$ gel to get the deposition precursor with $C_V = 0.013$ M. The $V_2O_5$ films were deposited on the fluorine doped tin oxide (FTO) coated glass at a voltage of −2.4 V. The as-deposited films were ambient dried and then annealed at 500 °C for 1 h in air.

---

* Corresponding author. Tel.: +1 206 616 9084; fax: +1 206 543 3100.
*E-mail address:* gzcao@u.washington.edu (G. Cao).

1388-2481/$ – see front matter © 2011 Elsevier B.V. All rights reserved.
doi:10.1016/j.elecom.2011.08.024

The surface morphology of porous $V_2O_5$ films was observed using scanning electron microscopes (SEM, JEOL, JSM-5200), and phase and crystallite size were studied using X-Ray Diffraction (XRD, Philips 1820 X-Ray Diffractometer). Surface area was determined by nitrogen adsorption–desorption at 77 K (NOVA 4200e, Brunauer–Emmett–Teller (BET)). Electrochemical properties of the $V_2O_5$ thin film electrodes were tested using a standard three-electrode setup. The cyclic voltammograms (CV) and chronopotentiometric (CP) measurement were performed using electrochemical analyzer (CH Instruments, Model 605B) in the voltage range of 0.6 V to −1.1 V (Vs. Ag/Ag$^+$) with 1 M $LiClO_4$ in propylene carbonate (PC) as electrolyte, a Pt plate as the counter electrode, and Ag/AgCl as the reference electrode.

## 3. Results and discussion

Porous $V_2O_5$ films were successfully fabricated by electrodeposition as shown in the SEM images in Fig. 1(a–b). The porous $V_2O_5$ films compose of homogeneously distributed pores of less than 100 nm in diameter, as well as $V_2O_5$ size of around 100 nm. Previously we have reported electrodeposition of folded $V_2O_5$ film electrodes from $V_2O_5$ sol using the similar method [9]. Block copolymer P123 has been reported as porous structure directing agents due to its amphiphilic properties, [10,11] and it could also reduce or prevent the aggregation of nanocrystallites as well as impede the crystal coarsening [12]. In this research, P123 is homogeneously mixed with $V_2O_5$ sol, where the vanadium species, e.g. $[VO_2]^+$, $VO_2$, $V_2O_5\ nH_2O$, could be anchored to the surfactant chain on P123 by the combined electrostatic force and hydrogen bonding in a low-pH aqueous solution [13]. After induced gelation and film formation by applying an external electrical voltage, the P123-templated vanadium oxide films could be homogeneously deposited onto FTO substrates. P123 was then removed by annealing the film in the air at 500 °C for 1 h. The specific surface area of the porous nanostructured $V_2O_5$ films was found to be ~40 m$^2$/g as determined by nitrogen sorption isotherms, which is larger than the surface area of porous structured $V_2O_5$ electrodes reported recently [14]. The macropores and ~100 nm $V_2O_5$ discernible from SEM images could not solely account for such a large surface area; in fact the surface area could mainly come from mesopores with pore size distribution centered at a diameter of 3.68 nm from BET result.

Fig. 1(c) shows the XRD patterns for the pristine porous $V_2O_5$ film and after the films intercalated with 0.76 mol and 1.18 mol Li$^+$ respectively. The porous $V_2O_5$ film annealed at 500 °C shows pure orthorhombic phase and the crystallite size is calculated to be 26.9 nm from the (001) peak based on Scherrer's equation, which is 8.2 nm smaller than the crystallite size of 35.1 nm in the folded structured $V_2O_5$ film electrodeposited from P123-free precursor[9]. The reduced crystallite size could be ascribed to the presence of P123 during film deposition and annealing, where it could effectively impede the crystal growth. The lattice constant along *c*-axis has also been calculated from (001) peaks in XRD patterns to be 4.32 Å, 4.39 Å and 4.67 Å for $V_2O_5$, $Li_{0.76}V_2O_5$ and $Li_{1.18}V_2O_5$ respectively. During Li$^+$ insertion/extraction in $V_2O_5$, Li$^+$ travels along the *b*-direction between $V_2O_5$ layers, which induces the buckled $V_2O_5$ planes, and reduces *a* and *b*-constants due to the reduction in repulsive Coulumbic force along the *ab*-plane. In the meantime, *c*-constant increases as the result of expansion of interlayer distance. The change in *c*-constant in this study is in good consistency with previous literatures [15].

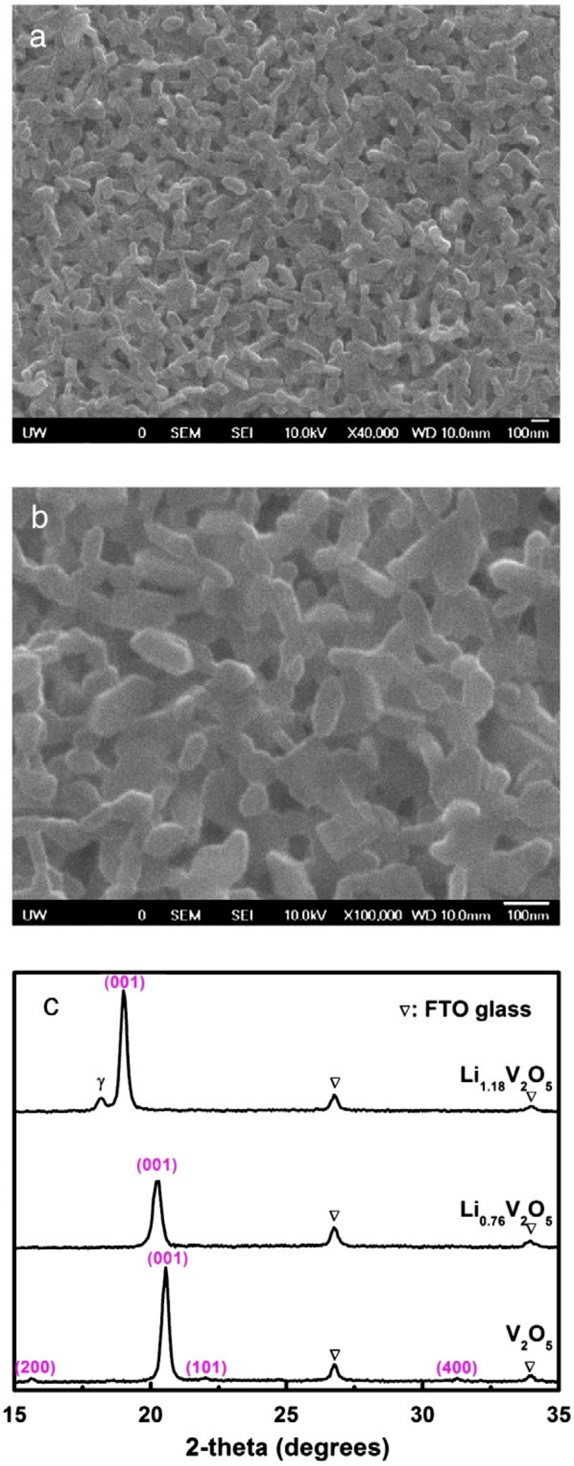

**Fig. 1.** (a) and (b) SEM images of 500 °C annealed porous $V_2O_5$ film on FTO glasses; (c) XRD patterns of porous $V_2O_5$ film before and after Li$^+$ intercalation. The crystallite size (26.9 nm) calculated from XRD peak is smaller than the $V_2O_5$ size (~100 nm) observed from SEM images, it is likely that SEM shows a secondary aggregated/stacked structure of small crystallites. In combination with BET result, the surface of small crystallites are accessible, therefore it is possible that electrolyte could penetrate through macropores and mesopores, resulting in more intercalation sites at the interface between electrolyte and electrode.

Fig. 2(a) shows the first 2 cycles of the cyclic votammogram (CV) of porous nanostructured $V_2O_5$ film electrodes when tested in 0.6 V to −1.1 V (*Vs*. Ag/Ag$^+$). The three pairs of redox peaks in Fig. 2(a) correspond to the reversible phase transitions among the following four Li$^+$ intercalated phases $Li_xV_2O_5$: α ($x<0.1$), ε ($0.35<x<0.7$), δ ($0.9<x<1$) and γ ($1<x<2$) [16]. Those successive phase transitions were also exemplified in the chronopotentiometric (CP) curves by the presence of three consecutive plateaus in Fig. 2(b). It can be calculated that the discharge capacity loss between the first and second cycle was 43 mAh/g, which could be mainly due to the existence of partial phase transition from γ phase to ω phase as marked in Fig. 2(b). From both the CV diagrams and CP curves, it can be

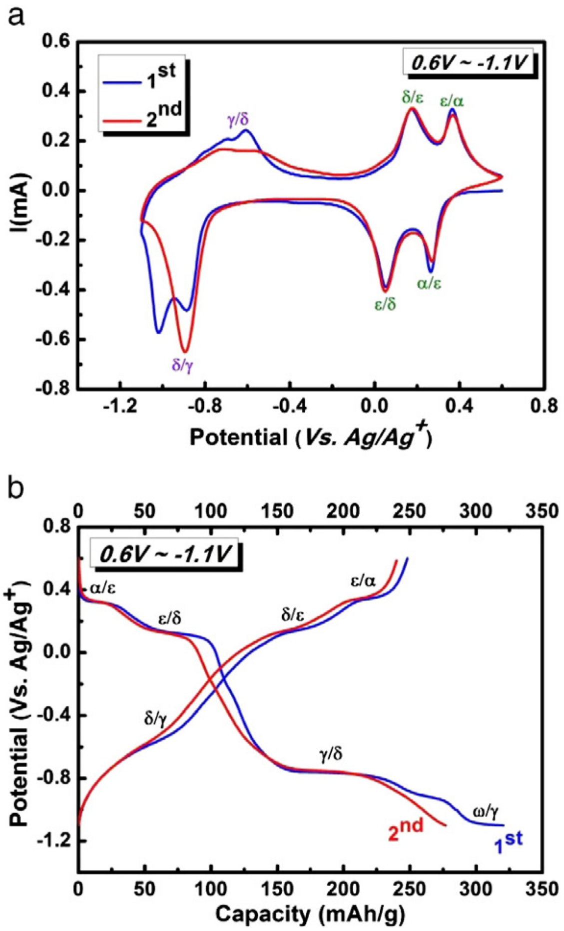

**Fig. 2.** (a) The cyclic voltammograms of 150 nm thick porous $V_2O_5$ films at 0.6 V to − 1.1 V (*Vs.* $Ag^+$/Ag) (scan rate: 2 mV/s) and (b) chronopotentiometric curves for discharge and charge process of 150 nm thick porous $V_2O_5$ film cathodes at 0.6 V to − 1.1 V (*Vs.* $Ag^+$/Ag) (current density: 180 mA/g).

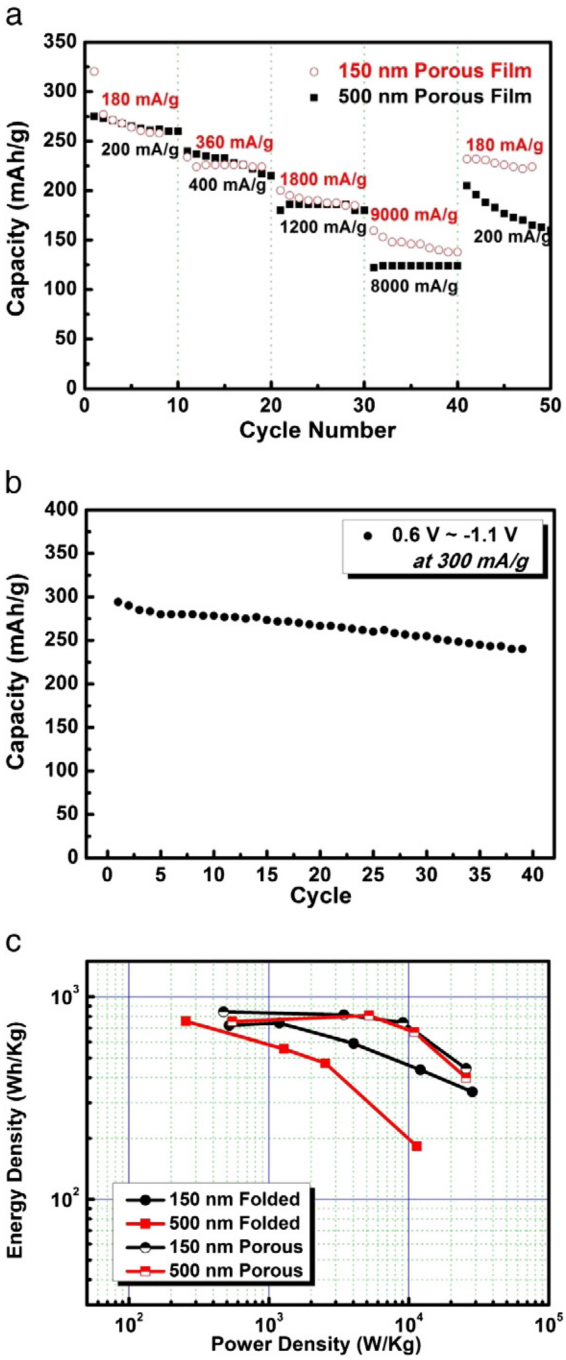

**Fig. 3.** (a) The rate performance of 150 nm and 500 nm thick porous $V_2O_5$ film cathodes at various current densities; (b) The cyclic performance of 150 nm porous $V_2O_5$ thin film cathodes at a current density of 300 mA/g for 40 cycles. (c) Ragone Plots comparing the energy densities and power densities of porous and folded structured films with different thickness.

concluded that the porous $V_2O_5$ films show a good reversibility when discharged and charged at 0.6 V to − 1.1 V (*Vs.* Ag/$Ag^+$).

Fig. 3(a) compares the discharge capacities of porous $V_2O_5$ films with different thicknesses when discharged consecutively at various discharge/charge rates. The 150 nm porous $V_2O_5$ film delivers a high discharge capacity of over 300 mAh/g in the initial cycle. At the 27th cycle, when a high current density of 9 A/g was applied, the discharge capacity maintains high as 160 mAh/g. When the thickness of the porous $V_2O_5$ film is increased to 500 nm, it still keeps an excellent rate capability with a discharge capacity of 124 mAh/g at 8 A/g as shown in Fig. 3(a). Fig. 3(b) shows the cyclic stability test at a constant current density of 300 mA/g for 40 cycles for porous $V_2O_5$ film with 150 nm in thickness. The initial discharge capacity was measured to be 294 mAh/g, and it stays as high as 240 mAh/g at the 40th cycle. The porous structure with $V_2O_5$ nanocrystallites together could offer a benign micro-environment with sufficient flexbility to accommodate volume change during $Li^+$ insertion and extraction, so that a good electrochemical stability and mechanical integrity could be guaranteed after many cycles. Fig. 3(c) are the Ragone Plots comparing the power densities and energy densities of the porous and folded structured $V_2O_5$ films. The 150 nm and 500 nm porous films show high energy density of 843 Wh/kg and 755 Wh/kg respectively, and high power density both of 25.6 kW/kg. The 500 nm folded film shows the worst properties both as in low energy density and power density. The difference of battery performance in altered film structures with various thicknesses could be ascribed to the following rationales. The unique structure in porous films could guarantee a large surface area with sufficient contact between electrode materials and electrolyte, which provides adequate intercalation sites for efficient $Li^+$ intercalation simultaneously. The presence of block copolymer P123 can delay the solid state diffusion and impede fine $V_2O_5$ nanocrystallites from agglomeration and coarsening during film formation and growth, therefore a short and fast $Li^+$ diffusion channel during phase propagation could be guaranteed. Whereas for the folded structured films, they could possess large surface area for efficient $Li^+$ intercalation when the films are as thin as 150 nm. However for the thicker folded films, they could become denser, partially losing the features of highly folded nanostructure and also the $V_2O_5$ particles could grow larger. The denser films are not able to offer sufficient penetration for electrolyte into all $V_2O_5$ particles, thus the $Li^+$ intercalation into thick $V_2O_5$ films would rely on and be bottlenecked by slow solid state $Li^+$ diffusion within large $V_2O_5$ particles during battery discharge. Similar phenomena of electrochemical performance degradation with increasing film thickness have also been reported in other literatures [17].

## 4. Conclusion

The porous nanostructured $V_2O_5$ films have been fabricated via a simple and low-cost electrodeposition approach from block copolymer P123 containing $V_2O_5$ precursor. P123 is believed to promote the formation of porous structure during film formation. Such $V_2O_5$ films demonstrated excellent electrochemical properties because porous $V_2O_5$ nanocrystallites possess (1) high surface area permitting enhanced charge transfer kinetics at the interface, (2) efficient $Li^+$ diffusion (3) good electrochemical stability and mechanical integrity.

## Acknowledgements

This research work has been financially supported in part by Nation Science Foundation (CMMI-1030048) and Pacific Northwest National Laboratories (PNNL).

## References

[1] J.M. Tarascon, N. Recham, M. Armand, J.N. Chotard, P. Barpanda, W. Walker, L. Dupont, Chem. Mater. 22 (2010) 724–739.
[2] D. Liu, G. Cao, Energy Environ. Sci. 3 (2010) 1218–1237.
[3] S.W. Oh, S.T. Myung, S.M. Oh, K.H. Oh, K. Amine, B. Scrosati, Y.K. Sun, Adv. Mater. (2010) 4842–4845.
[4] D.H. Wang, D.W. Choi, J. Li, Z.G. Yang, Z.M. Nie, R. Kou, D.H. Hu, C.M. Wang, L.V. Saraf, J.G. Zhang, I.A. Aksay, J. Liu, ACS Nano 3 (2009) 907–914.
[5] H. Zhang, X. Yu, P.V. Braun, Nat. Nanotechnol. 6 (2011) 277–281.
[6] K. Takahashi, Y. Wang, G.Z. Cao, J. Phys. Chem. B 109 (2005) 48–51.
[7] D.W. Liu, Y.Y. Liu, B.B. Garcia, Q.F. Zhang, A.Q. Pan, Y.H. Jeong, G.Z. Cao, J. Mater. Chem. 19 (2009) 8789–8795.
[8] N. Meethong, Y.H. Kao, S.A. Speakman, Y.M. Chiang, Adv. Funct. Mater. 19 (2009) 1060–1070.
[9] Y.Y. Liu, M. Clark, Q.F. Zhang, D.M. Yu, D.W. Liu, J. Liu, G.Z. Cao, Adv. Energy Mater. 1 (2011) 194–202.
[10] X. Li, X. Wang, H. Chen, P. Jiang, X. Dong, J. Shi, Chem. Mater. 19 (2007) 4322–4326.
[11] D. Zhao, J. Feng, Q. Huo, N. Melosh, G.H. Fredrickson, B.F. Chmelka, G.D. Stucky, Science 279 (1998) 548–552.
[12] Q. Wu, W. Li, Y. Cheng, Z. Jiang, Mater. Chem. Phys. 91 (2005) 463–467.
[13] R. Jiang, T. Huang, J. Liu, J. Zhuang, A. Yu, Electrochim. Acta 54 (2009) 3047–3052.
[14] R.N. Reddy, R.G. Reddy, J. Power Sources 156 (2006) 700–704.
[15] S. Hub, A. Tranchant, R. Messina, Electrochim. Acta 33 (1988) 997–1002.
[16] C. Delmas, H. Cognac-Auradou, J.M. Cocciantelli, M. Ménétrier, J.P. Doumerc, Solid State Ionics 69 (1994) 257–264.
[17] K. Le Van, H. Groult, A. Mantoux, L. Perrigaud, F. Lantelme, R. Lindström, R. Badour-Hadjean, S. Zanna, D. Lincot, J. Power Sources 160 (2006) 592–601.